Internal Transitions of Negatively Charged Magnetoexcitons and Many Body Effects in a Two-Dimensional Electron Gas

H. A. Nickel, T. M. Yeo, A. B. Dzyubenko,* B. D. McCombe, and A. Petrou
Department of Physics and Center for Advanced Photonic and Electronic Materials, SUNY Buffalo, Buffalo, New York 14260

A. Yu. Sivachenko
Department of Physics, University of Utah, Salt Lake City, Utah 84112

W. Schaff
School of Electrical Engineering, Phillips Hall, Cornell University, Ithaca, New York 14853

V. Umansky
Department of Condensed Matter Physics, The Weizmann Institute of Science, 76100 Rehovot, Israel
(Received 27 October 2000; revised manuscript received 21 August 2001; published 16 January 2002)

Internal transitions of quasi-two-dimensional, negatively charged magnetoexcitons (X^-) and their evolution with excess electron density have been studied in GaAs/AlGaAs quantum wells. In the dilute electron limit, due to magnetic translational invariance, the optically detected resonance spectra are dominated by bound-to-continuum bands in contrast to the negatively charged donor system D^-, which exhibits strictly bound-to-bound transitions. With increasing excess electron density Landau-level filling factors $\nu < 2$ the X^--like transitions are *blueshifted;* they are absent for $\nu > 2$. The blueshifted transitions are explained in terms of a new type of collective excitation — magnetoplasmons bound to a mobile valence band hole.

DOI: 10.1103/PhysRevLett.88.056801 PACS numbers: 73.20.Mf, 71.70.Di, 76.40.+b, 78.90.+t

Since the initial observation of negatively charged excitons X^- in quantum wells (QWs) [1], there has been considerable interest in *charged electron-hole* (e-h) *complexes* in quasi-two-dimensional (quasi-2D) semiconductor systems. The negatively charged exciton, like its atomic physics analog, the negatively charged hydrogen ion H^-, provides a central example of the role of *electron-electron correlations* in a Coulomb potential. However, X^- in QW structures is different in several important respects: (1) The positively charged holes have a mass comparable to the electron mass; (2) the magnetic field energy can dominate at laboratory magnetic fields; (3) the system is quasi-2D; (4) the density of excess electrons N_e in the wells can be controlled (at low N_e, X^- is the *stable ground state* of the photoexcited carrier system). Additionally, in contrast to one-component electron systems with free carriers or carriers in a parabolic confining potential [2,3], the corrections to the single-particle states are directly measurable by *intraband* optical experiments.

The evolution with N_e of the electron-hole (e-h) system in quasi-2D structures from isolated neutral excitons via X^- to a few-hole/many-electron plasma and also the effects of a magnetic field have been studied by interband methods [4–9]. At zero field the X^- feature evolves with increasing N_e into the Fermi edge of the e-h plasma [10]; the density at which the crossover takes place depends on the inherent disorder in the sample [4]. When the electrons and holes are confined in the same spatial region along the growth direction, the magnetophotoluminescence (magneto-PL) or magnetoabsorption changes abruptly with increasing magnetic field at Landau-level (LL) filling factor $\nu = 2$ from band-gap renormalized LL-to-LL–like transitions ($\nu > 2$) to "excitonlike" behavior ($\nu < 2$) irrespective of N_e. The nature of the excitonlike states for $\nu < 2$ remains not well understood [6], and the *interband* measurements alone cannot distinguish between a collective, many body state and a dilute X^- system (see [7,9], and references therein). Internal excitonic transitions (IETs), which are now understood for neutral [11,12] and charged [13] excitons, probe directly the ground and excited state properties, and thus can be used for investigating the excitonic state in the dilute situation and its evolution with N_e and magnetic field.

The X^- complex, although superficially similar to the negatively charged donor D^- [14,15], differs in one very important respect: the positive charge in X^- is mobile. A symmetry associated with the resulting center-of-mass (c.m.) motion (magnetic translational invariance) leads to a new, exact electric-dipole selection rule that *prohibits* internal transitions between certain families of X^- states [16]. In particular, the spin-singlet and -triplet bound-to-bound transitions that dominate the spectra of D^- [14,15] are *strictly forbidden* for X^-. The present experimental observation and studies of internal transitions of X^- in GaAs QWs as functions of N_e and magnetic field provide new insight into this complex system. At low N_e bound-to-bound transitions are absent, and both singlet and triplet features appear as continuous bands,

with positions in quantitative agreement with numerical calculations. At high N_e and low fields ($\nu > 2$) *internal transitions are not observed*; in contrast, for $\nu < 2$ they appear but are *blueshifted* in energy from their low-N_e counterparts. These experiments (1) verify the predicted consequences of the magnetic translational symmetry [16], and (2), more importantly, clearly show that the feature identified as X^- for $\nu < 2$ represents the *collective response* of a few-hole/many-electron system.

The exact selection rules for IETs of isolated charged excitons [16] are shown in Fig. 1a. In the strictly 2D high-field limit the only family (of macroscopically degenerate) bound states associated with the lowest $n_e = 0$, $n_h = 0$ LL is the triplet X^-_{t00} [17–19]. The X^- states are properly specified in magnetic fields [16] by the total electron spin S_e ($S_e = 0$ for singlet, s, and $S_e = 1$ for triplet, t, states), by the hole spin S_h ($S_{hz} = \pm 3/2$ for heavy holes), by the total angular momentum projection m_z, and by the discrete oscillator quantum number $k = 0, 1, \ldots$ (related to the center of rotation of the complex). Because of macroscopic LL degeneracy in k, X^- states form degenerate families. Each family starts with its $k = 0$ parent state (solid dots in Fig. 1a), which has a specific value of angular momentum projection, $m_z^{k=0}$, determined by particulars of the interactions. The degenerate daughter states $k = 1, 2, \ldots$ have angular momentum projections $m_z = m_z^{k=0} - k$ (open dots in Fig. 1a). In the next electron LL ($n_e = 1$, $n_h = 0$), there is also only one (macroscopically degenerate) bound triplet state, X^-_{t10} [16]. In contrast to D^- [14], the X^- eigenstates consist of discrete bound states *and* continua (due to the extended c.m. motion of the neutral magnetoexciton) and, in general, the far-infrared (FIR) spectra include both bound-to-bound and bound-to-continuum transitions. The bound-to-bound transition $X^-_{t00} \rightarrow X^-_{t10}$ (dotted arrow in Fig. 1a) is allowed by the usual selection rules ($m_z \rightarrow m_z + 1$ for σ^+ polarization, spin conserved). This is the analog of the strong T^- transition for the D^- center [14,15]; it lies *below* the electron cyclotron resonance (e-CR) in energy. For X^-, however, the *additional exact selection rule* $\Delta k = 0$ must also be satisfied, reflecting the fact that the center of rotation of the complex in **B** cannot be displaced by the absorption of a photon propagating along the field direction. Because the c.m. and internal motions are coupled in **B**, k and m_z are not independent, and *both* selection rules cannot be satisfied simultaneously for the bound-to-bound transition, $X^-_{t00} \rightarrow X^-_{t10}$. The oscillator strength is transferred to bound-to-continuum transitions (T_1 and T_2 in Fig. 1a). In addition to a magnetoexciton band of width $E_0 = \sqrt{\pi/2}\, e^2/\epsilon l_B$, $l_B = (\hbar c/eB)^{1/2}$, extending below each LL and describing a $1s$ exciton plus a scattered electron in the corresponding LL ($X_{00} + e_0$ and $X_{00} + e_1$), the continuum of three particle states (hatched regions) also includes a band of width $0.57E_0$ below the first excited electron LL. The latter corresponds to an excited ($2p^+$) exciton plus a scattered electron in the zero LL ($X_{10} + e_0$). Transitions to the $X_{00} + e_1$ continuum are dominated by a sharp onset at the edge (energy of e-CR plus the X^- binding energy: solid arrow T_1 in Fig. 1a (see also Fig. 1b). In addition, there is a broader, weaker peak associated with transitions to the lower edge of the $X_{10} + e_0$ magnetoexciton band (dashed arrow T_2). Detailed calculations show that these qualitative triplet features remain at finite fields and confinement, *and also hold for the singlet* X^- *states,* which form the ground state [19] at low and intermediate fields. The singlet counterparts of the triplet transitions T_1 and T_2 (see Fig. 1a) are denoted below as S_1 and S_2.

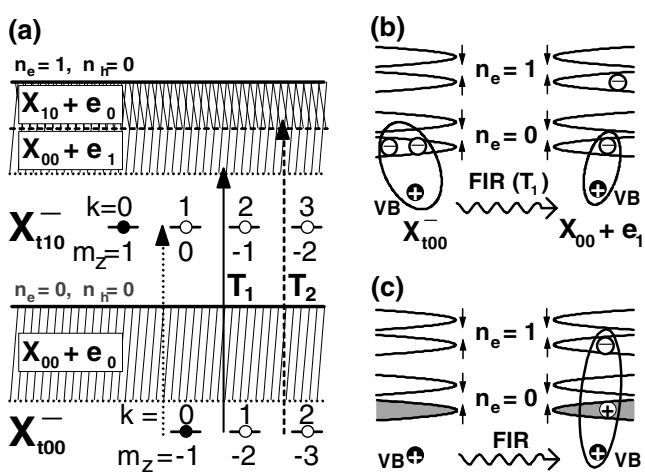

FIG. 1. Schematic diagram of (a) the X^--triplet energy states associated with the two lowest electron Landau levels for the strictly 2D, high magnetic field limit. Initial and final states in the FIR transition (b) for the isolated X^- and (c) for electron filling factor $\nu = 1$.

Four GaAs/$Al_{0.3}Ga_{0.7}As$ multiple quantum well samples grown by molecular beam epitaxy were investigated. Samples 1 and 2 are nominally undoped with (20 nm) GaAs wells and $Al_{0.3}Ga_{0.7}As$ barriers: sample 1—20 wells with 60 nm barriers; sample 2—10 wells with 20 nm barriers. Samples 3 and 4 have 24 nm wells and are Si doped in the central third of the $Al_{0.3}Ga_{0.7}As$ barriers at sheet densities of 8×10^{10} and 2.8×10^{11} cm^{-2}, respectively: sample 3 (4)—20 (10) wells with 48 nm (24 nm) barriers. The FIR absorption resonances in a magnetic field were studied by optically detected resonance (ODR) spectroscopy [12]. Electrons, holes, and excitons were continuously created by optical excitation with the 632.8 nm line of a He-Ne laser coupled to the sample (at low temperature in the Faraday geometry in the center of a 15/17 T superconducting magnet) through an optical fiber; PL was collected via a second fiber [20]. Photoexcited exciton densities are estimated to be approximately 10^7 cm^{-2} at an excitation laser intensity of 100 mW/cm^2.

Raw ODR data for sample 1 are shown in Fig. 2a; Fig. 3a shows a summary of the triplet and singlet ODR

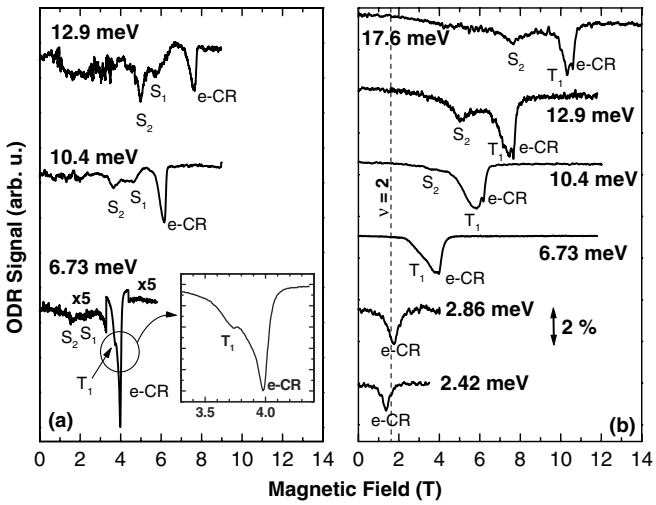

FIG. 2. ODR spectra for (a) sample 1 and (b) sample 3. The features labeled S_1, S_2, and T_1 refer to the internal singlet and triplet transitions of X^- discussed in the text.

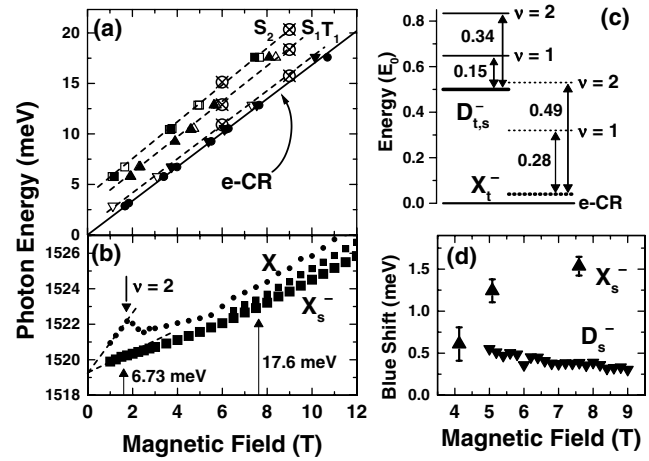

FIG. 3. (a) Summary plot for samples 1 (closed symbols) and 2 (open symbols): internal singlet S_1 (▲, △), S_2 (■, □), and triplet T_1 (▼, ▽) transitions of X^-. Open circles with crosses: numerical calculations. Dashed lines are guides to the eye. (b) Magneto-PL for sample 3 from the ground and excited X^- states (■): At $B \sim 7$ T the two different hole spin states are resolved. The highest energy line (●) above 6 T is the neutral exciton, X. Band-gap renormalized LL-to-LL transitions (linear in B) are seen below 1.8 T. Up arrows denote the expected field positions for the S_2 transition at the indicated photon energies (Fig. 2b). (c) Calculated energies (in units of $E_0 = \sqrt{\pi/2}\, e^2/\epsilon l_B$) of magnetoplasmons bound to D^+ and h^+. The heavy solid and dotted lines indicate the transition energies for the isolated, strictly 2D, $D^-_{t,s}$ and X^-_t states, respectively. Blueshifts are indicated by double-headed arrows. (d) Experimental blueshift in X^- singletlike (▲) and D^- singletlike (▼) [22] transitions.

data from the two undoped samples 1 and 2. The ODR signal obtained by tracking the X^--PL feature (Fig. 3b) is plotted vs magnetic field at several FIR laser photon energies. Very similar, but positive-going, ODR spectra are obtained by tracking the X-PL line. The sharp feature at 6.3 T at 10.4 meV is e-CR. Three features are attributed to X^- internal transitions (S_1, S_2, and T_1); similar features are seen in sample 2. The weak shoulder at fields just below e-CR is ascribed to the dominant triplet ionizing transition T_1. The peak of this band corresponds to the edge of the continuum, so the observed peak is shifted to higher energies from e-CR by the (small) triplet binding energy, with a tail at higher energies (lower fields). Quantitative numerical calculations for a 20 nm GaAs QW, performed using an expansion in LL's incorporating size quantization [14], are shown in Fig. 3a at 6 and 9 T by the circles with crosses. We estimate the absolute accuracy achieved in determining the X^- binding energies to be 0.1–0.2 meV with no adjustable parameters [21]. The agreement with experiment is excellent and provides quantitative support for the assignment of the observed features [13].

The clearest signature of the new physics associated with the magnetic translational invariance is the X^--triplet transition. The bound-to-bound transition (dotted arrow in Fig. 1a) should occur on the *high-field* (low-energy) side of the e-CR. There is *no indication* of a line at this position in the ODR data of Fig. 2. The strongest feature seen near e-CR is a broad band on the *low-field* side, precisely as predicted for the allowed and strong [16] bound-to-continuum triplet transition of X^-, T_1.

To explore the effects of large densities of excess electrons and the interesting behavior of the magneto-PL above and below $\nu = 2$ we have also investigated modulation-doped samples under very similar conditions. ODR results for sample 3 ($N_e = 8 \times 10^{10}$ cm^{-2}) are shown in Fig. 2b; in this case the only PL feature seen at low temperature and low fields evolves into an X^--like line for $\nu < 2$ (Fig. 3b). It is clear from Fig. 2b that, for laser photon energies of 6.73 meV and above, the ODR band just below the sharp e-CR (the triplet band T_1) is now much stronger than it is for low N_e and is also shifted to lower magnetic fields (a blueshift in energy). The large width of this band is also apparent. At this density, filling factor $\nu = 2$ occurs at $B \simeq 1.6$ T. At smaller photon energies, for which the resonant field would lie below that of $\nu = 2$, there is no evidence of this triplet band, and the e-CR line is broader and symmetric. Note also that the *dominant* singletlike line S_2, which at low N_e corresponds to the $X^-_s \rightarrow X_{10} + e_0$ transition, is clearly seen at the two highest laser photon energies, for which the resonance occurs at fields corresponding to $\nu < 2$. This feature loses strength at a photon energy of 10.4 meV, and is not observable at 6.73 meV and below (resonant fields corresponding to $\nu > 2$).

The data for sample 4 are similar, except that, due to the higher density, the singletlike S_2 and tripletlike T_1 bands are observable only at fields above 5 T ($\nu = 2$ at 5.8 T). Features observed in samples 3 and 4 occur at lower fields than the corresponding features in the nominally undoped samples—they are *blueshifted* in energy. This measured blueshift of the dominant X^- feature S_2 is shown in Fig. 3d along with data [22] for the D^- singlet blueshift [23] for

a well- and barrier-doped sample of approximately equal dimensions and N_e.

The blueshift is the signature of a many-electron phenomenon; the relevant collective excitations are magnetoplasmons. In the absence of the valence band hole, they are characterized by the conserved center-of-mass momentum $\mathbf{K}$ and are neutral bound e-h pairs [24]. Because of Kohn's theorem [2], only $\mathbf{K} = 0$ magnetoplasmons with the bare e-CR energy $\hbar\omega_{ce}$ are FIR active. In the presence of the valence band hole, the final states are *charged mobile e-h* complexes in a magnetic field [7,16] (see Fig. 1c). The interaction with the valence band hole mixes various $\mathbf{K}$ states, obviating Kohn's theorem; many states acquire oscillator strength. Our calculations for 2D systems with integer filling factors $\nu = 1, 2$ show that there is one prominent absorption peak in the region of energies larger than $\hbar\omega_{ce}$; it corresponds to a *magnetoplasmon bound to the mobile hole* h^+. These excitations resemble the magnetoplasma modes bound to the *fixed* donor ion D^+ in the presence of many electrons [23], but the magnetic translational invariance is broken for the latter. Energies of bound collective modes experience discontinuities at integer ν (cf. [7,23]) and increase with increasing ν, reflecting the enhanced contribution of the exchange-correlation effects and explaining the blueshift. As seen in Fig. 3d the measured blueshifts for the singlet X^- with the *mobile* hole are, somewhat surprisingly, *larger* than those for the D^- for fields above 5 T. This is in qualitative agreement with theory for the blueshift of the X^- triplet internal transition (see Fig. 3c). The larger blueshift for the X^- results from the diminished negative contribution of the Coulomb e-h interaction to the final state energy for the mobile hole. We conclude that "X^--like" PL features seen in QWs with excess electrons at $\nu < 2$ represent a collective response of the electron-hole system, which gradually approaches the isolated X^- for $\nu \ll 1$.

This work was supported in part by NSF DMR 9722625 and by a COBASE grant. We are grateful to the Center for Computational Research at UB for providing the supercomputer facilities.

*On leave from General Physics Institute, RAS, Moscow 117942, Russia.

[1] K. Kheng *et al.,* Phys. Rev. Lett. **71**, 1752 (1993).
[2] W. Kohn, Phys. Rev. **123**, 1242 (1961).
[3] J. Dempsey and B. I. Halperin, Phys. Rev. B **45**, 1719 (1992).
[4] G. Finkelstein, H. Shtrikman, and I. Bar-Joseph, Phys. Rev. Lett. **74**, 976 (1995).
[5] A. J. Shields *et al.,* Phys. Rev. B **51**, 18 049 (1995).
[6] D. Gekhtman *et al.,* Phys. Rev. B **54**, 10 320 (1996).
[7] P. Hawrylak and M. Potemski, Phys. Rev. B **56**, 12 386 (1997).
[8] R. T. Cox *et al.,* Acta Phys. Pol. A **94**, 99 (1998).
[9] E. I. Rashba and M. D. Sturge, Phys. Rev. B **63**, 045305 (2001).
[10] V. Huard *et al.,* Phys. Rev. Lett. **84**, 187 (2000).
[11] R. H. M. Groeneveld and D. Grishkowski, J. Opt. Soc. Am. B **11**, 2502 (1994).
[12] M. S. Salib *et al.,* Phys. Rev. Lett. **77**, 1135 (1996); J. Černe *et al.,* Phys. Rev. Lett. **77**, 1131 (1996); J. Kono *et al.,* Physica (Amsterdam) **249B–251B**, 527 (1998); H. A. Nickel *et al.,* Phys. Rev. B **62**, 2773 (2000).
[13] A. B. Dzyubenko *et al.,* Physica (Amsterdam) **6E**, 156 (2000).
[14] A. B. Dzyubenko and A. Yu. Sivachenko, Phys. Rev. B **48**, 14 690 (1993).
[15] Z. X. Jiang *et al.,* Phys. Rev. B **56**, R1692 (1997).
[16] A. B. Dzyubenko and A. Yu. Sivachenko, Phys. Rev. Lett. **84**, 4429 (2000).
[17] A. Wojs and P. Hawrylak, Phys. Rev. B **51**, 10 880 (1995).
[18] J. J. Palacios, D. Yoshioka, and A. H. MacDonald, Phys. Rev. B **54**, R2296 (1996).
[19] D. M. Whittaker and A. J. Shields, Phys. Rev. B **56**, 15 185 (1997).
[20] J. Kono *et al.,* Phys. Rev. B **52**, R8654 (1995).
[21] An iteration procedure similar to that of [19] was used for picking out a relatively large but limited subspace (several thousand basis elements) of the total Hilbert space, so as to maximize the projection of the true eigenstate. The following parameters for the 20 nm $GaAs/Al_{0.7}Ga_{0.3}As$ QW were used: isotropic effective electron mass $m_e = 0.067$, in-plane (perpendicular) hole mass $m_{h\|} = 0.24$ ($m_{h\perp} = 0.34$), dielectric constant $\epsilon = 12.5$, total band-edge discontinuity $\Delta U = \Delta U_e + \Delta U_h = 352$ meV with a ratio $\Delta U_e/\Delta U_h = 70{:}30$.
[22] J. G. Tischler, Ph.D. thesis, SUNY, Buffalo, 2000.
[23] J.-P. Cheng *et al.,* Phys. Rev. Lett. **70**, 489 (1993); A. B. Dzyubenko and Yu. E. Lozovik, JETP **77**, 617 (1993); P. Hawrylak, Phys. Rev. Lett. **72**, 2943 (1994).
[24] Yu. A. Bychkov, S. V. Iordanskii, and G. M. Eliashaberg, JETP Lett. **33**, 143 (1981); C. Kallin and B. I. Halperin, Phys. Rev. B **30**, 5655 (1984).